Article

Quantitative Detection of the Influenza a Virus by an EGOFET-Based Portable Device

Elena Y. Poimanova [1], Elena G. Zavyalova [1,2], Elena A. Kretova [1], Anton A. Abramov [1], Askold A. Trul [1], Oleg V. Borshchev [1], Anna K. Keshek [1,2], Sergey A. Ponomarenko [1,2] and Elena V. Agina [1,3,*]

[1] Enikolopov Institute of Synthetic Polymeric Materials of Russian Academy of Sciences, Profsoyuznaya Str. 70, 117393 Moscow, Russia; poymanova@ispm.ru (E.Y.P.); zlenka2006@gmail.com (E.G.Z.); e.kretova@ispm.ru (E.A.K.); abramov@ispm.ru (A.A.A.); trul@ispm.ru (A.A.T.); borshchev@ispm.ru (O.V.B.); akeshek@list.ru (A.K.K.); ponomarenko@ispm.ru (S.A.P.)
[2] Chemistry Department, Lomonosov Moscow State University, Leninskiye Gory 1/3, 119991 Moscow, Russia
[3] Department of Fundamental Physical and Chemical Engineering, Lomonosov Moscow State University, Leninskiye Gory 1/3, 119991 Moscow, Russia
* Correspondence: agina@ispm.ru

Abstract: Elaboration of biosensors on the base of organic transistors with embedded biomolecules which can operate in an aqueous environment is of paramount importance. Electrolyte-gated organic field-effect transistors demonstrate high sensitivity in detection of various analytes. In this paper, we demonstrated the possibility of quantitative fast specific determination of virus particles by an aptasensor based on EGOFET. The sensitivity and selectivity of the devices were examined with the influenza A virus as well as with control bioliquids like influenza B, Newcastle disease viruses or allantoic fluid with different dilutions. The influence of the semiconducting layer thickness on EGOFETs sensory properties is discussed. The fabrication of a multi-flow cell that simultaneously registers the responses from several devices on the same substrate and the creation of a multi-sensor flow device are reported. The responses of the elaborated bioelectronic platform to the influenza A virus obtained with application of the portable multi-flow mode are well correlated with the responses obtained in the laboratory stationary mode.

Keywords: biosensor; EGOFET; aptamer; virus detection; multi-flow chamber

1. Introduction

Inexpensive, time-saving and reliable for rapid testing sensor platforms for ions and biological substances in situ detection in appropriate media attract the ever-growing interest of researchers and consumers [1–4]. Since a liquid electrolyte is an ideal medium for biomolecules, the elaboration of biosensors on the basis of organic transistors with embedded biomolecules that can operate in an aqueous environment is of paramount importance. Electrolyte-gated organic field-effect transistors (EGOFETs) are very promising for this purpose. They capture increasing attention due to their ability to transduce sensory signals, providing direct electrical response to label-free biorecognition events at a low voltage. At the same time, they meet the requirements of device miniaturization, fast data acquisition and processing [5–7].

The response of a bio-recognizing EGOFET can be evaluated with the convenient method of measuring the device transfer characteristics in the saturated or linear region [5]. Main extracting parameters that determine the quality and performance of EGOFETs as well as can play a role of sensory response are source-drain current (I_{DS}), field-effect mobility (or transconductance, g_m), gating system capacitance (C_i), and threshold voltage (V_{th}) [5,6].

EGOFETs can form two electric double layers. Therefore, they operate as capacitors with high specific capacitance at very low voltages (<0.5 V), which allows detection of various biomarkers in water media and bio-fluids [8]. Even very slight changes of the

EGOFET interfaces lead to the shifts of electric parameters, allowing to detect extremely small amounts of the target analyte [9]. The gate or semiconductor surface modification by biorecognition elements provides sensitivity and specificity of the device [5,10,11]. It is worth mentioning that these label-free biosensor platforms have shown detection limits in the picomolar or even zeptamolar range [9,12]. It has been proven that the reproducibility error, estimated as a relative standard deviation for more than a hundred repeated measurements, is just a few percent [13].

EGOFET-based specific detection of analytes requires sensor functionalization with recognition elements, e.g., nucleic acid aptamers, antibodies, etc. Nucleic acid aptamers are artificial structured oligonucleotides (from 15 to 100 nucleotides in length) with high affinity and specificity to the target analyte. Aptamers can be selected to bind various targets, including cations, organic compounds, proteins, viruses and cells. Chemical synthesis of the aptamers allows site-specific modifications with fluorophores, anchors, chelators etc. that are useful for creation of complex multifunctional constructs. Additionally, DNA and especially modified nucleic acid aptamers have high stability in both biological and non-physiological media. All these properties promote engaging the aptamers as therapeutics and recognition elements in sensors [10,14–17].

Examples of successful implementation of the aptamers in biosensors (the so called "aptasensors") can be illustrated by the detection of viruses [10,18,19]. Aptamers are compatible with a variety of analytical approaches, for example, colorimetry, fluorescence assay, surface plasmon resonance, surface-enhanced Raman spectroscopy, electrochemical detection, and field-effect transistors [18]. Aptasensors are able to detect a few viral particles in the sample with the limit of detection of 10–100 viral particles per mL or 2–5 viral particles per sample within 15 min [20]. Although these characteristics are outstanding, the development of aptasensors is ongoing in order to simplify the production of sensors and corresponding equipment for the signal acquisition. Together with the possibility of using cheap glass or flexible polymer substrates and due to the fact that it is a label-free detection method, the fabrication of an EGOFET-based aptasensor for detecting viruses in a wide range of concentrations is very promising for the creation of point-of-care devices that can compete with the existing analogues. In this paper, we upgrade the previously elaborated approach in order to reach not only rapid specific detection of virus particles but the possibility of its quantitative determination using an EGOFET-based aptasensor separately and within a multi-flow chamber.

2. Materials and Methods

Materials

Organic semiconductors that form the active semiconducting layers of two types of EGOFET platforms—2,7-dioctyl-benzothieno [3,2-b][1]benzothiophene (C8-BTBT-C8) and 1,3-bis{11-(7-heptyl [1]benzothieno [3,2-b][1] benzothio-2-yl)hexyl}-1,1,3,3-tetramethyl-disiloxane (BTBT-dimer)—were synthesized according to the described routes in [6,21], respectively. Synthesis of the biotin-containing derivative of dialkyl-benzothienobenzothiophene (Und-BTBT-Hex-biotin, BTBT-biotin) required for biotinylation of the bioreceptor layer, was synthesized according to the route described in [10].

Streptavidin (SA) and Bovine Serum Albumin (BSA), DNA aptamer RHA0385 (5′–biotin-TTGGGGTTATTTTGGGAGGGCGGGGGTT–3′) were purchased from Sigma-Aldrich. The influenza A virus, Newcastle Disease virus (NDV), influenza B virus and allantoic fluid were provided by the Chumakov Federal Scientific Center for Research and Development of Immune and Biological Products of the Russian Academy of Sciences. The biopreparation details are provided in Supplementary Materials and in [20].

Fabrication of EGOFET Devices

The C8-BTBT-C8 and PS were mixed using the weight ratio of 4:1 [22] and dissolved in toluene to receive a total concentration of 18 mg mL^{-1}. The blend deposition was made with Doctor Blade coater Film Applicator Coatmaster 510 (Erichsen, Hemer, Germany) at

85 °C as described in [6,23] and resulted in fabrication of a thick (40 nm) film of the organic semiconductor layer.

BTBT-dimer solution in toluene (C = 0.33 mg/mL) was prepared and used for the Langmuir–Schaeffer OSC layer fabrication technique as described in [21] and resulted in fabrication of a thin (several monolayers) film of the OSC layer. Data were collected with a Nima 712BAM system (Nima, Coventry, UK) using a Teflon trough and barriers at room temperature. An interface layer of PS from toluene solution (C = 3.6 mg/mL) was deposited by Doctor Blade on the substrate with electrodes before Langmuir–Schaeffer BTBT-dimer film fabrication.

BTBT-dimer (C = 0.33 mg/mL, toluene) and BTBT-biotin (C = 0.33 mg/mL, dimethyl-sulfoxide) were mixed in a weight ratio of 19:1 and deposited using the Langmuir-Schaeffer technique to fabricate a biosensor with 5% BTBT-biotin on the surface without the OS sublayer. The ratio of BTBT-dimer: BTBT-biotin equal to 7:3 was used to fabricate the biorecognition layer with 30% of BTBT-biotin on the surface on the thin or thick OS layers. This technique of biorecognition layer fabrication was described earlier in [10]. An interface layer of PS from toluene solution (C = 3.6 mg/mL) was deposited by Doctor Blade on the substrate with electrodes before Langmuir–Schaeffer BTBT-dimer/5% BTBT-biotin film fabrication.

PDMS reservoir was manufactured from Ecoflex 0–50 rubber using the method described in [6].

Thin-Film Characterization

The formation of semiconducting and biorecognition layers was controlled by atomic force microscopy (NT-MDT Solver Next, Moscow, Russia) in a tapping mode under ambient conditions using NT-MDT HA-FM silicon probes with a resonant frequency of 77 kHz.

Biosensing measurements

Electrical measurements of the biosensors were performed at normal conditions using a Keithley 2634B (Tektronix, Beaverton, OR, USA) source-meter and a probe station PS-100 (Printeltech LLC, Moscow, Russia). Extraction of the EGOFET's electrical characteristics was made by transfer curves fitting in the voltage range that corresponds to saturation regime [5,6,10] using Shockley's equation.

Virus determination

The biosensing layers were fabricated on the base of the EGOFETs with a bioreceptor layer by subsequent treation by the following way: (1) Streptavidin immobilization (100 mg L^{-1} solution in 1 g L^{-1} BSA solution in PBS during 10 min, then wash with PBS and H_2O; (2) Biotinylated RHA0385 aptamer immobilization during 5 min, then wash with PBS and H_2O.

Biosensing was performed by immobilization of modified EGOFETs to a biological liquid: virus of influenza A (H7N1 strain, 6.1×10^9 virus particles per mL diluted by PBS in the proportion of 1/10; 1/100; 1/1000; 1/10,000; 1/100,000) or control viruses (B/Victoria/2/1987, 6.1×10^9 virus particles per mL, Newcastle Disease virus, 3.6×10^9 virus particles per mL) or allantoic fluid, all diluted by PBS in the proportion of 1/100; 1/10,000. After 10 min incubation washing with PBS and with H_2O.

The above-mentioned procedure provides specific binding of every layer. The examination of the influence of non-specific interactions on the biosensor performance was provided in [10].

Flow chamber measurements

The flow chamber developed in previous work [6] was used to perform stability measurements of the biosensor based on EGOFET in the constant flow of liquid and also for virus detection with flow chamber. The sample placing into the flow chamber was similar to the process described in [6]. The difference was in the measurement source-meter: in this work we used only portable source-meter, described in Section 3.5.

3. Results and Discussion

3.1. Biosensor Fabrication Technique

Organic semiconductors organosilicon BTBT-dimer and C8-BTBT-C8 were chosen for the biosensors fabrication due to their chemical stability in air and in aqueous media, both under conventional lighting, as well as their high field-effect mobility in OFETs [21,24] and EGOFETs [6,10]. The blend of C8-BTBT-C8 and polystyrene dissolved in toluene was deposited on a glass substrate using the Doctor Blade technique. Due to phase microsegregation promoted by high temperature, polystyrene precipitates on the surface of the substrate and C8-BTBT-C8 forms the top layer. The device architecture is schematically depicted in Figure 1a. By this approach the EGOFET device with a thick OSC film previously estimated to be 40 nm was fabricated [23].
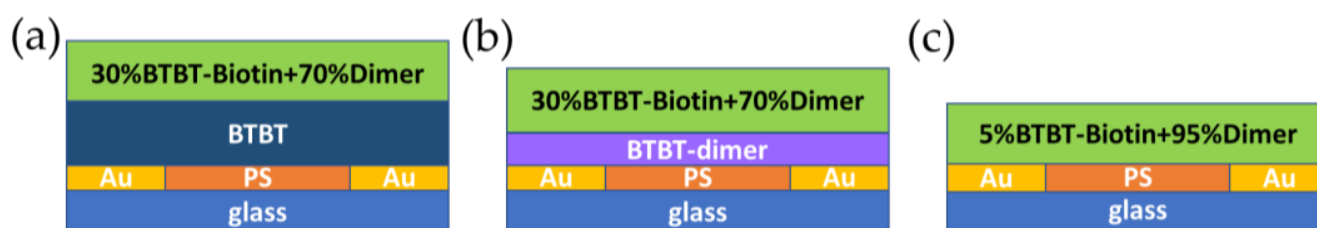
Figure 1. The architecture of the EGOFET-based biosensor devices manufactured with different OSC sublayers: (**a**) C8-BTBT-C8; (**b**) BTBT-dimer; (**c**) without any OSC sublayer.

It was shown in our previous papers that organosilicon derivatives of non-symmetric dialkyl-BTBT derivatives provide large-area charge-transporting thin layers of the OSC, which leads to outstanding sensing properties of the OFETs [25]. However, the sensing mechanism of EGOFETs and OFETs differs. That is why it was interesting to check the influence of the thickness of an OSC layer for EGOFET-based biosensors. Using C8-BTBT-C8 and the BTBT-dimer in this work provides an approximate ratio of the OSC thicknesses for C8-BTBT-C8: BTBT-dimer as 4:1. EGOFETs based on the BTBT-dimer were fabricated by Langmuir–Schaefer technique that utilizes the amphiphilic nature of BTBT-dimer. It contains the hydrophilic siloxane anchor group, which can form hydrogen bonds with a water surface promoting the stable Langmuir film formation and hydrophobic alkyl chains which can form an ordered layer which improves the operational stability of the device [26]. It is worth mentioning that the Doctor Blade and Langmuir–Schaeffer techniques are scalable and thus suitable for low-cost fabrication that is especially significant for creation of portable devices for affordable widespread use of point-of-care (POC) applications [27]. The device architecture with the BTBT-dimer layer is schematically depicted in Figure 1b.

Each of two described types of the EGOFETs containing twenty separate transistors (for stationary Probe Station measurements) or five separate transistors (for flow-chamber measurements) on the same substrate were subsequently modified by application of a biorecognition layer. The desired functionality of the biorecognition layer, deposited above the semiconducting layer by using the Langmuir–Schaefer technique, was achieved using the blend of a siloxane dimer of BTBT (BTBT-dimer) and a biotin derivative of BTBT (BTBT-biotin). The last one contains a terminal biotin fragment in the structure, which provides anchor for bioanalytes on the surface of OSC. Formation of the functional biotinylated film does not significantly influence the performance of EGOFETs with OSCs of C8-BTBT-C8 and BTBT-dimer sublayers, but at the same time provides the location of the biorecognition sites very close to the current-carrying layer [10]. The composition of the biorecognition layer was optimized earlier and contains 30% of BTBT-biotin in the film, providing enough sites for steric placement of streptavidin molecules that is extremely significant for further immobilization of the target biomolecules, namely aptamers and viruses in this work.

The third type of the devices investigated consists of the biorecognition layer only without an OSC sublayer and was fabricated to apply the concept of extra high sensitivity typical for the very thin semiconducting layer in OFET-based devices [25] to the EGOFET

ones. Previously, it was established that the device with 30% of the BTBT−biotin-based bioreceptor layer only and contains no active OSC layer shows low electrical properties with low current region and low stability due to a small thickness of the layer [10].

In this work the concentration of BTBT-biotin in the biorecognition layer was decreased to 5% in order to stabilize the device performance keeping in mind that the second component of this layer, BTBT-dimer, serves as an OSC, and there are several publications on its OFET properties [21,26]. At the same time, it was shown in [10] that the device with the C8-BTBT-C8 OSC layer and biorecognition layer containing 5% of BTBT-biotin is sensitive to the virus of influenza A. However, the response shift is worse than that of the biorecognition layer containing 30% of BTBT-biotin. Tuning of the OSC layer thickness could improve the sensitivity of the 5% BTBT-biotin containing device. Therefore, the device with 5% BTBT-biotin in the biorecognition layer was fabricated without any OSC sublayer. The device architecture with the biorecognition layer only is schematically depicted in Figure 1c.

The formation of all functional layers of the devices was controlled by AFM microscopy. The morphology images of the biorecognition layer on the surfaces of three types of devices are shown in Figure 2. All of them are typical for thin films of BTBT-containing molecules as it was published earlier [10,23] and non-dependent on the OSC sublayer.
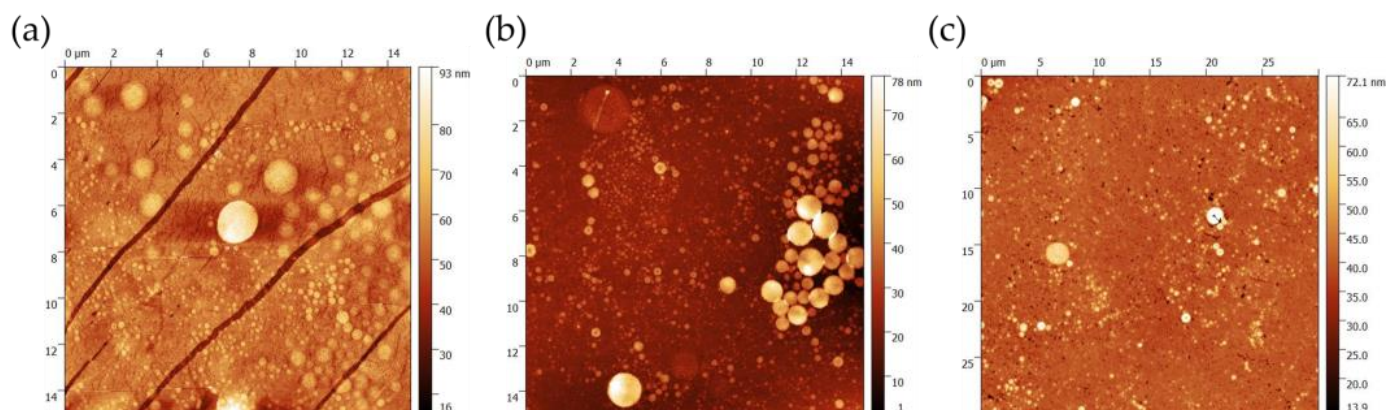
Figure 2. AFM scans of the surface of the EGOFET-based biosensor devices manufactured with different OSC sublayers: (**a**) C8-BTBT-C8; (**b**) BTBT-dimer; (**c**) without OSC sublayer.

3.2. Electrical Characteristics of Three Types of EGOFETs with a Biorecognition Layer

All fabricated EGOFETs having a biorecognition layer on the top of a semiconducting layer demonstrate good electrical characteristics including low hysteresis and high stability during measurement and under storage both in deionized water or PBS solution or in air atmosphere under conventional indoor lighting. All architectures of the devices show good electrical performance including a high on-off ratio, transconductance and low threshold voltage. The electrical parameters of three types of devices examined are summarized in Table 1. They are averaged on 60 devices for each type of device. The transfer characteristics of the EGOFETs recorded in deionized water in the saturated mode are provided in the Supplementary Materials (Figure S1). In contrast to the device without an OSC layer with a biorecognition layer containing 30% of BTBT-biotin [10], only the device with 5% of BTBT-biotin operates adequately for EGOFETs (averaged over 20 samples).

Table 1. Electrical parameters of biosensor devices manufactured with different OSC layers (averaged on 60 devices).

Device	I_{on}, µA	I_{off}, nA	g_m, A$^{1/2}$ V^{-1}($\times 10^6$)	V_{th}, mV
C8-BTBT-C8/biorecognition layer with 30%BTBT-biotin	-0.11 ± 0.02	-0.01 ± 0.004	-3.5 ± 0.5	-215 ± 50
BTBT-Dimer/biorecognition layer with 30%BTBT-biotin	-0.35 ± 0.05	-0.05 ± 0.006	-6.3 ± 0.7	-235 ± 30
Biorecognition layer with 5%BTBT-biotin	-0.10 ± 0.03	-0.01 ± 0.005	-3.4 ± 0.6	-112 ± 20

Notes: I_{on}—the on current; I_{off}—the off current; g_m—the transconductance; V_{th}—the threshold voltage.

3.3. Detection of Specific and Non-Specific Interactions with Virus Particles

Further development of biorecognition properties of the fabricated devices was based on the streptavidin-biotin interactions. The recognition element used for specific binding with analyte was represented by DNA aptamer RHA0385 due to its ability to bind different strains of the influenza A virus with nearly the same affinity [28,29], allowing for the detection of independent strains of the virus [28,30]. Both types of EGOFETs—having the OSC sublayer and the 30% BTBT−biotin containing biorecognition layer—perform good electrical characteristics, as shown by well-shaped transfer curves (Figure 3a,b) demonstrating acceptable on/off current ratio after all biomolecules loading.
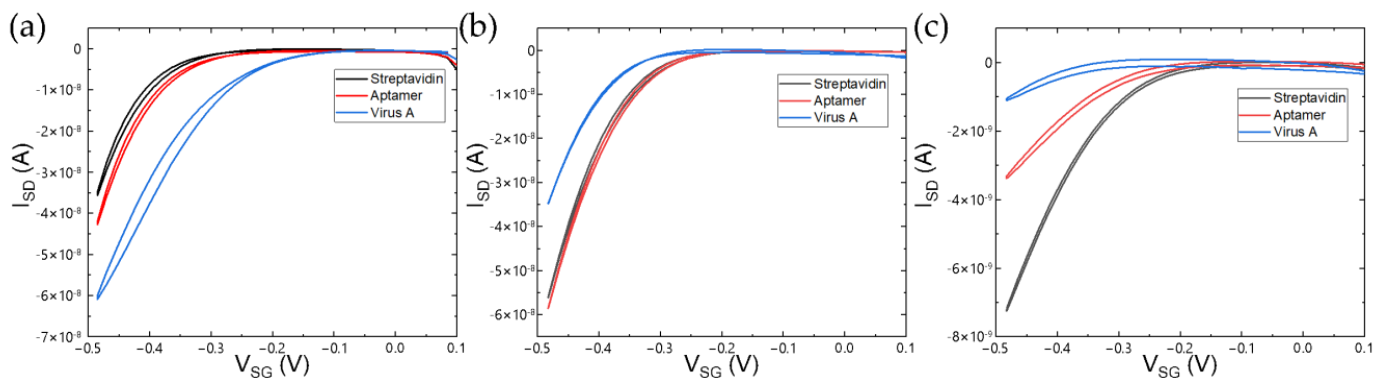
Figure 3. Transfer characteristics of the devices with different OSC sublayers: (**a**) C8-BTBT-C8; (**b**) BTBT-dimer; (**c**) without an OSC sublayer.

Concerning the third type of biosensor, unfortunately, the concept of the combination of stability-sensitivity parameters improving by decreasing the BTBT-biotin content and decreasing the OSC layer thickness (while this approach in OFETs leads to significant improvements) did not work. A device with the third architecture, containing only 5% of the BTBT-biotin layer did not possess good reproducibility, showing degradation of the electrical characteristics. Therefore, it can be concluded that immobilization of biomolecules on a thin biorecognition layer deteriorates the EGOFET device performance (Figure 3c).

It is demonstrated that the influence of OCS presence in the bio-EGOFET with the OCS surface modified by a biorecognition layer is significant in terms of the charge transport during sensing. It was shown for the third device without the OSC sublayer that the biorecognition layer with the reduced biotin-content itself can work as a transistor. However, it undergoes strong degradation during the loading of the subsequent layers of biomolecules. Therefore, the second device could be considered roughly like a thicker

biorecognition layer due to the similar composition of the OSC and functional layer—both the biorecognition layer and OSC-dimer contain BTBT-dimer, the latter in the case of the second device provides better charge transport and more stable work than the third device with biorecognition layer containing 5% of BTBT-biotin. As it was shown in [10], the device with 30% of the BTBT-biotin based bioreceptor layer and without an active OSC layer shows low electrical properties with the values of currents lying in the nA region and low stability, which is not suitable for the EGOFET application. It can be concluded that almost all charge transport in the first type of device occurs by the C8-BTBT-C8 OSC layer.

3.4. Effect of the Active Layer Organic Semiconductor Material and LOD of the Devices

To assess the possibility of quantitative bioanalyte determination using EGOFETs with two different OSC active layers, experiments with the virus of influenza A diluted in the range of five orders were conducted (Figure 4a,b). Specificity of the detected device response to the target sensing event instead of non-specific binding at the transistor channel that could generate false positive or negative responses, was confirmed by conducting several control experiments. To evaluate the specificity, the control virus NDV, influenza B virus or virus-free biological fluid was assayed in the presence of the bioreceptor layer covered with streptavidin and biotinylated aptamer. It was found that control fluids do not induce any significant transconductance variation (Figure 4c,d). Therefore, the influenza A virus-induced increase in the transconductance within the investigated range of concentrations (Figure 4a,b) is a result of the electric transduction of highly specific interactions within the active surface of the device. All the devices measured showed reproducible electrical characteristics and very low degradation during the measurements. The limit of detection (LOD) of influenza A virus was estimated as the response that is 3 times higher than the standard deviation (over 10 replicates) measured in the reference solution and it was equal to 6.1×10^5 viral particles per mL for the first type of device with the C8-BTBT-C8 thick OSC layer and 6.1×10^4 viral particles per mL for the second type of device with the BTBT-dimer thin OSC layer. Comparing the normalized parameter g_m(aptamer)/g_m(virus of influenza A) values one can notice that the device with the OSC layer based on the BTBT-dimer has a nearly 1.5 times higher response to the virus of influenza A.

The LOD of 6.1×10^4 viral particles per mL and time of virus detection experiment below 15 min place the sensor in a row of rapid tests for virus determination. The gold standard of rapid diagnostics of the influenza A virus in point-of-care applications is antibody-based test strip (lateral flow immunoassay) with LOD of 1×10^6–1×10^8 viral particles per mL and time of analysis of 10–15 min [31]. Our setup has at least a 1.5-fold lower LOD with the same time of the experiment. The lowest LOD is achieved by the polymerase chain reaction with reverse transcription (RT PCR) with character LOD values in the range of 3×10^2–1.2×10^3 influenza A viral particles per mL, but the time of analysis is 2–3 h [32,33]. These characteristics place RT PCR in a row of laboratory tests outside of point-of-care applications. Loop-mediated isothermal amplification assay with reverse-transcription (RT LAMP) is an intermediate solution in viral diagnostics having LOD of 10^4 influenza A viral particles per mL and time of analysis about 1 h [34]. Our sensor is 4-time less time consumable having sufficient LOD for practical application. The typical viral load in human samples, e.g., swabs, is in the range of 10^5–10^8 influenza A genomes per mL [35] that is nearly equivalent to 10^5–10^8 influenza A viral particles per mL. This range of viral loads is completely covered with proposed aptasensor (Figure 4).

Both sensors demonstrated excellent specificity in determination of the influenza A virus as compared to off-target viruses and virus-free biological fluid. The high specificity of the RHA0385 aptamer has been shown previously [20]. These new results indicate a low level of non-specific binding to the aptamer placed on the EGOFET surface demonstrating good coverage of the hydrophobic layer consisting of BTBT-derivatives by the hydrophilic layer made up of macromolecules (streptavidin and DNA aptamer). The specificity was achieved without any detergents and extensive washing steps that simplify the procedure.
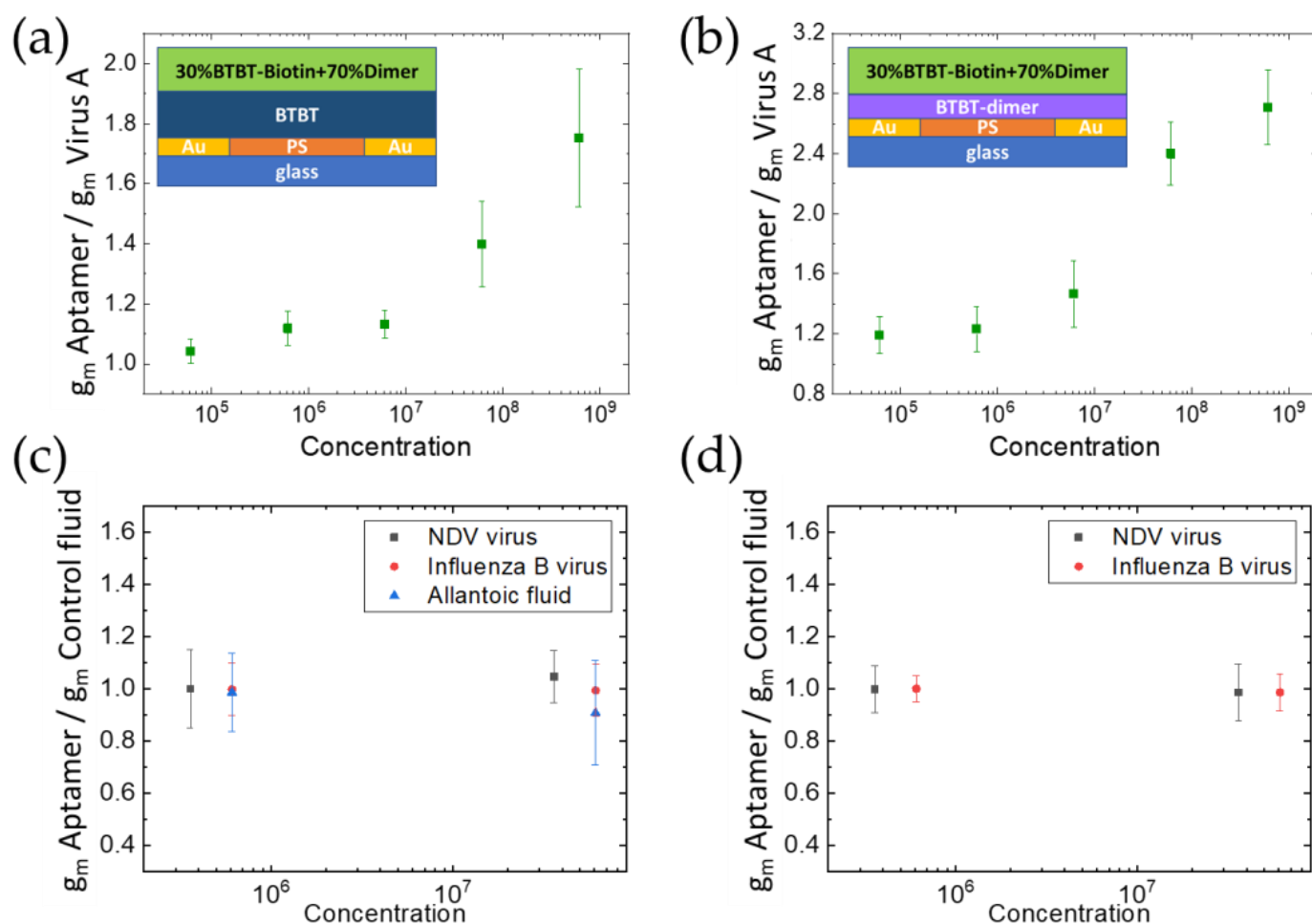
Figure 4. The limit of detection of virus of influenza A by the devices with C8-BTBT-C8 (**a**) and BTBT-dimer (**b**) semiconducting layers and biotin-containing receptor layers. Results of control experiments with the control virus NDV, virus of influenza B or virus-free biological (allantoic) fluid for C8-BTBT-C8 (**c**) and BTBT-dimer (**d**) containing devices.

### 3.5. Portable Device Fabrication and Virus Detection with Multi-Flow Chamber

The combination of an array of biosensors, a microfluidic analyte delivery system, and an electronic data analysis unit makes it possible to analyze biological fluids for the presence of complex biological molecules in real time with low resource costs [9,36,37].

To collect responses from an array of sensors, a measuring device was developed, as well as a sensor cell that performs electrical switching and connects the system for supplying the analyzed liquid. The multi-flow biosensor cell consists of the following elements: a printed circuit board with a gate electrode, a movable plate with several spring-loaded contacts for connecting to the drain and source electrodes, a spacer, a PDMS-seal, an upper clamping bar, and injection needles with fluoroplastic adapters for connecting silicone tubes (Figure 5). The close-up view photograph of the fabricated sensor chip can be found in the Supplementary Materials (Figure S2).

The measuring device is based on the STM32F373 microcontroller, which includes a 16-bit analog-to-digital converter with an input multiplexer, as well as a two-channel digital-to-analog converter. The analog part of the device consists of five transimpedance amplifiers for converting transistors' channels from currents to voltages, as well as two inverting amplifiers for supplying voltage to the gate and source of transistors. A bias voltage equal to half of the supply voltage is applied to the non-inverting inputs of the amplifiers in order to be able to supply voltages of both signs while using a unipolar supply. The built-in software of the device allows simultaneous measuring of the transfer and

output characteristics of five transistors on the substrate, while the drains of the transistors and the common gate are connected to the corresponding voltage sources, and each of the sources is connected to the input of the corresponding transimpedance amplifier.
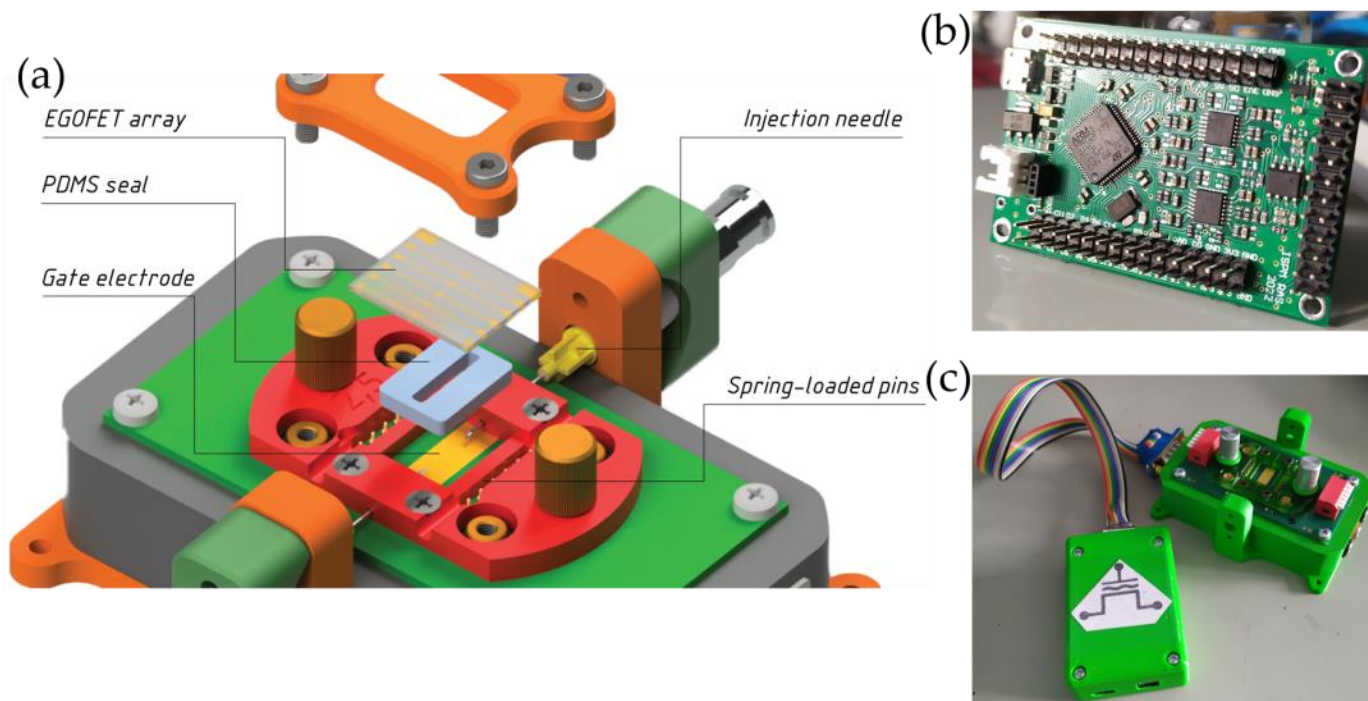

Figure 5. EGOFET-device in a flow mode: (**a**) exploded view of a flow cell. Photos of the measuring device from different sides (**b**,**c**).

To perform measurements, custom firmware was written in C programming language without using an operating system. The device communicates with custom PC applications through a USB interface set up as a virtual serial port. The application sends the command and measurement parameters such as timings and voltages to the device and listens for incoming data. The device performs measurement cycles until the stop command is received or measurement cycles are exceeded.

The microcontroller is clocked with 48 MHz clock from an internal crystal stabilized oscillator, and the internal ADC is clocked with 6 MHz, which allows for performing the conversion on all input channels in less than 500 us. The ADC is triggered by the timer with fixed frequency of 1 kHz, and after the conversion is complete, the result is transferred to the buffer in the RAM by the direct memory access controller. The data point to be sent is obtained from averaging of several conversions, a number of which is specified in measurement parameters. This configuration allows to free the core computational resources for sample processing and data transfer.

At startup ADC self-calibration sequence is launched, which is said to compensate for internal ADC offset and gain error. The external calibration is performed by means of a Keithley 2000 multimeter, attachable relay board and one resistor. The relay board connects one input channel at a time through the resistor and multimeter to the output of the voltage source of the device.

Calibration of channels for measuring the current and voltage source is carried out automatically using a switching board that connects any of the channels with a reference ammeter or voltmeter, and a special program on a PC that controls the device and the reference meter (Figure 6). The aim of the calibration is to calculate the coefficients of the linear equation, which relates DAC code and output voltage, or ADC code and input current. Thus, the offset and gain errors of the whole circuit are considered.
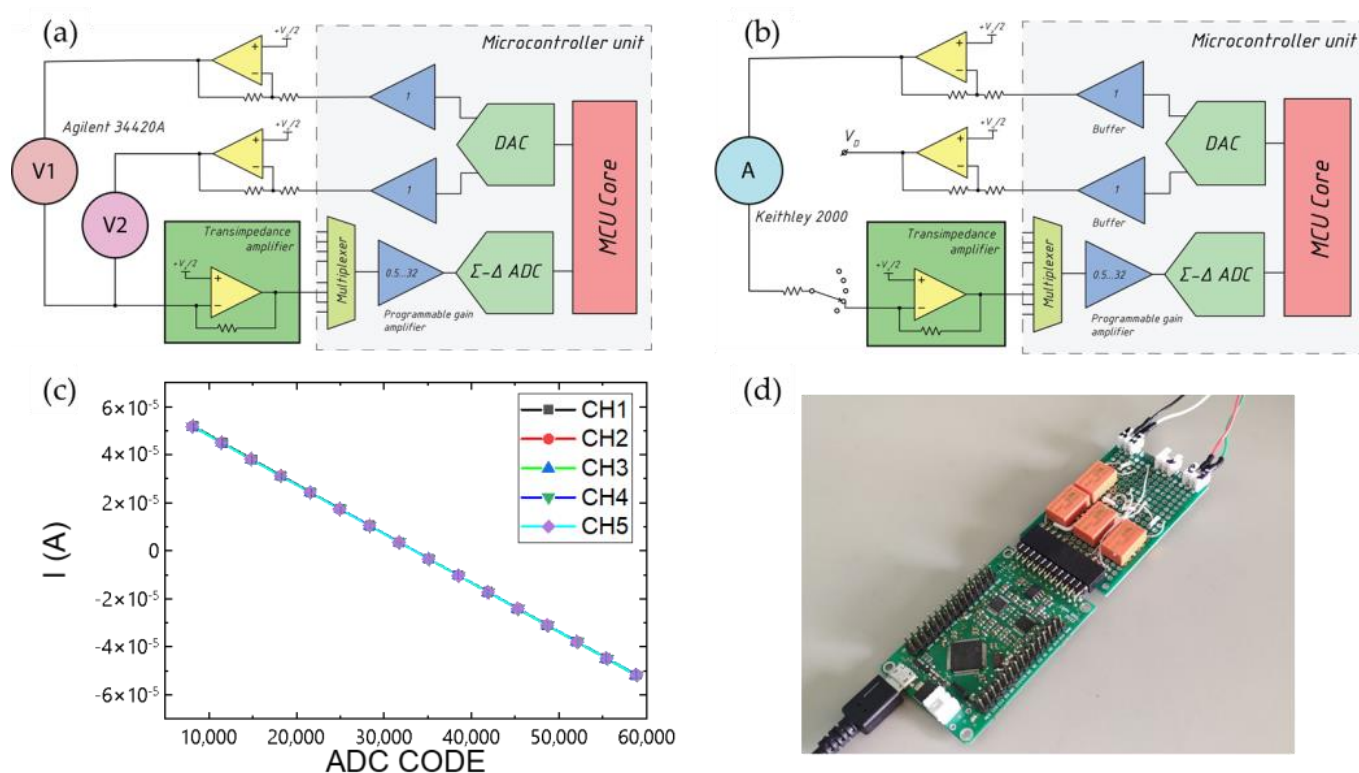
Figure 6. Schematic of the voltage source calibration circuit (**a**). Schematic for calibrating the current measurement channel (**b**). Current channel calibration plot (**c**). A photo of the switching board and the meter (**d**).

The first model of the flow chamber with the opportunity of single measurements was successfully used to detect the pH-changes in solutions [6]. The presented upgrade of the flow chamber allows for tracking the changes of several (five in this version) EGOFETs on the same sample that can provide an assessment of reproducibility and selectivity of the device response. Such an approach is also suitable for creation of a multisensory device.

An example of a handheld bioelectronics system based on EGOFETs with an extended gate for detection of the SARS-CoV-2 virus, spike S1, and immunoglobulin G antigen proteins in biofluids was reported by Macchia et al. [37]. The developed device BioScreen combines high sensitivity and portability. Nevertheless, the portable device provided in the present paper is suitable for the creation of a multisensory device for detection of several analytes within one sample that can be captured by the large-scale biorecognition layer based on biotin-streptavidin interaction. Proof-of-concept is provided.

To estimate the biosensor efficiency in a flow chamber mode, a stability test (cyclic measurements of the transfer characteristics, 1 transfer curve per 70 s) was performed for the first type of described devices (with C8-BTBT-C8 OSC layer, Figure 1a). Two hours of operation of the biotinylated EGOFET show a slight shift of the threshold voltage by 1.5% demonstrating very good stability of the device and ensuring the reliability during real-time measurements (Figure 7a). The devices with a biorecognition layer showed good electrical performance: high on-off ratio, transconductance, as well as a low threshold voltage (Figure 7b,c). The typical transfer characteristics of two EGOFET-devices recorded in DI water in parallel mode within the flow chamber are shown on Figure 7b, visually demonstrating the reproducibility of the response. Immobilization of the consequent layers of streptavidin, biotinylated aptamer, and the virus of influenza A leads to a shift of the electrical characteristics that can be seen on Figure 6c and demonstrates the same behavior of the biosensing platform as was established for measuring the response on a stationary Probe Station. The threshold voltage, similarly, to non-flow chamber experiments, shifts with good reproducibility that is shown on Figure 7d by the parameter

$(V_{th}(apt)\text{-}V_{th}(vir))/V_{th}(apt)$ calculation, where $V_{th}(apt)$—the threshold voltage, measured for the aptamer-modified device, $V_{th}(vir)$—the threshold voltage, measured for the virus of influenza A-treated device.
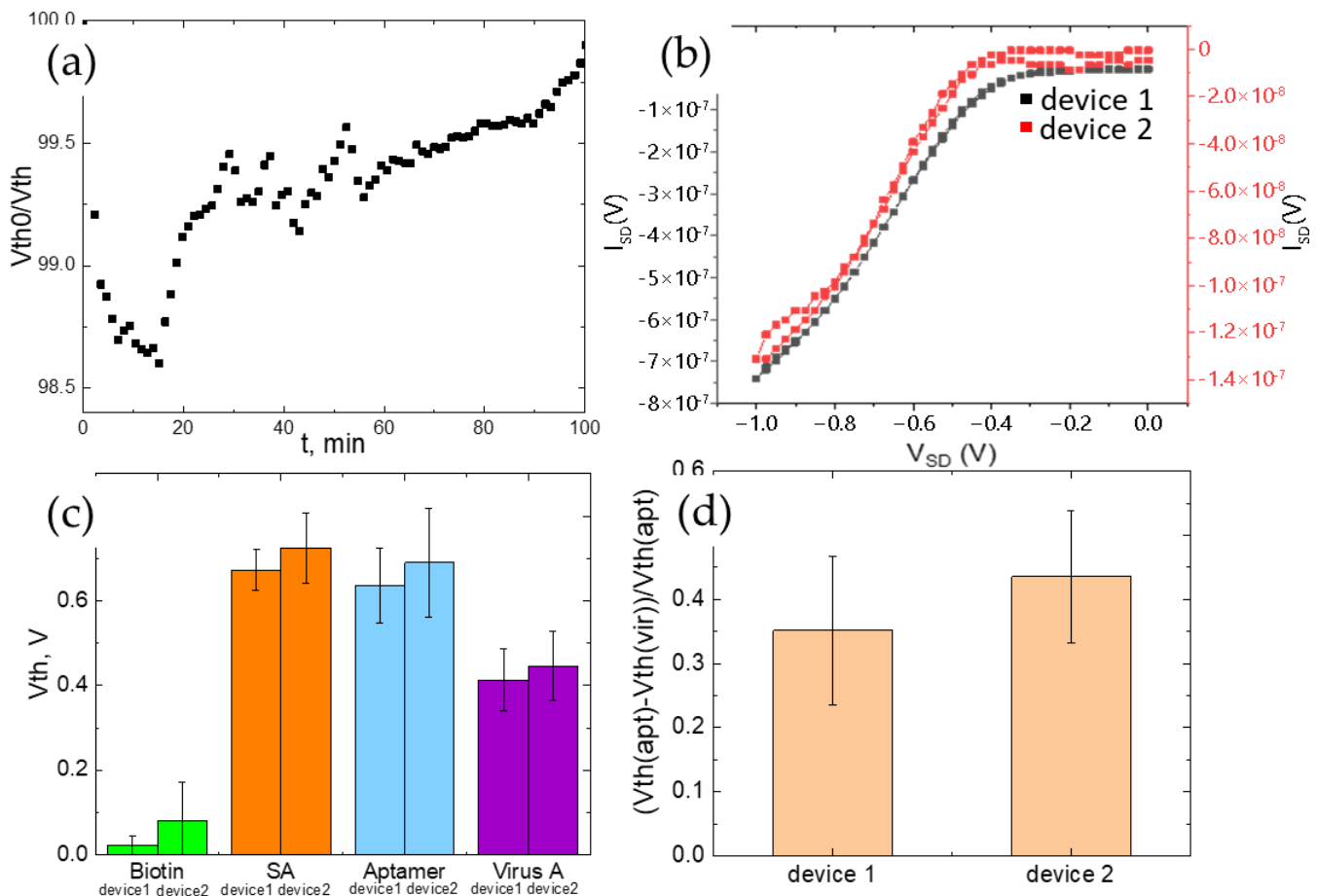
Figure 7. (**a**) Operation of the biotinylated EGOFET in the flow chamber; (**b**) The typical transfer characteristics of two EGOFET-devices recorded in DI water in parallel mode within the flow chamber; (**c**) Response of the biosensors to streptavidin, biotinylated aptamer, virus of influenza A; (**d**) Shift of the threshold voltage in sensing of virus of influenza A by RHA0385 aptamer.

4. Conclusions

To sum up, we developed the previously elaborated approach in order to reach both rapid specific detection of viral particles and quantification of the viral load using an EGOFET-based aptasensor that was demonstrated on the example of the influenza A virus. The high specificity of the devices fabricated was proved, providing statistically significant dose-dependent signals in the concentration range of 6×10^4–6×10^8 viral particles per mL of the influenza A virus on a par with no interfering signals in the presence of off-target viruses (influenza B virus and virus of Newcastle disease) or virus-free biological fluid (allantoic fluid). Limit of detection of influenza A virus up to 6.1×10^5 viral particles per mL was achieved for the first type of device with the C8-BTBT-C8 thick OSC layer and 6.1×10^4 viral particles per mL for the second type of device with the BTBT-dimer thin OSC layer. The influence of the semiconducting layer thickness on the sensory properties of EGOFETs was investigated and stated that the device based on a single biotinylated bioreceptor layer without an OS sublayer demonstrates sensitivity to the influenza A virus, but it is poorly reproduced while EGOFET devices with both thick and thin active semiconducting layers and a biotinylated bioreceptor layer demonstrate high sensitivity to the influenza A virus. The thinner organic semiconducting sublayer in bio-EGOFET demonstrates a more intense signal (1.5 times higher) to the virus and an order of magnitude of greater

sensitivity. A multi-flow cell that simultaneously registers the responses from several EGOFET devices on the same substrate was designed and fabricated. The responses of the elaborated bioelectronic platform to the influenza A virus obtained with application of portable multi-flow mode are well correlated with the responses obtained in laboratory stationary mode that paves the way to the creation of a multi-sensor flow device that can serve as a portable point-of-care device for differential diagnostics of various diseases.

Supplementary Materials: The following supporting information can be downloaded at: https://www.mdpi.com/article/10.3390/chemosensors11080464/s1, Figure S1. The typical transfer characteristics of epy EGOFET-based biosensor devices manufactured with different OSC sublayers: (a) C8-BTBT-C8; (b) BTBT-dimer; (c) without OSC sublayer. Figure S2. The photograph of the fabricated sensor chip with five EGOFETs on the one glass substrate (left) and polarizing optical microscopy microphotograph of separate EGOFET pixel with interdigitated electrodes covered by functional layers (right).

Author Contributions: Conceptualization, E.Y.P., E.G.Z. and E.V.A.; methodology, E.Y.P., E.G.Z., E.V.A. and S.A.P.; formal analysis, E.Y.P., E.G.Z., A.A.T., E.A.K. and A.K.K.; investigation, E.Y.P., E.G.Z., E.A.K., A.K.K., A.A.A. and O.V.B.; resources, E.A.K., A.K.K., A.A.A. and O.V.B.; writing—original draft preparation, E.Y.P., E.G.Z., A.A.A. and A.A.T., writing—review and editing, E.Y.P., E.G.Z., A.A.A., A.A.T., O.V.B., S.A.P. and E.V.A.; supervision, E.G.Z., S.A.P. and E.V.A.; project administration, E.V.A. All authors have read and agreed to the published version of the manuscript.

Institutional Review Board Statement: Not applicable.

Informed Consent Statement: Not applicable.

Data Availability Statement: The completed data of this study are available from the corresponding author.

Conflicts of Interest: The authors declare no conflict of interest.

References

1. Torricelli, F.; Manoli, K.; Macchia, E.; Torsi, L.; Magliulo, M. Electrolyte-gated organic transistors for biosensing applications. *Org. Sen. Mat. Appl.* **2016**, 71–105. [CrossRef]
2. Courtney, S.J.; Stromberg, Z.R.; Myers y Gutiérrez, A.; Jacobsen, D.; Stromberg, L.R.; Lenz, K.D.; Theiler, J.; Foley, B.T.; Gans, J.; Yusim, K.; et al. Optical Biosensor Platforms Display Varying Sensitivity for the Direct Detection of Influenza RNA. *Biosensors* **2021**, *11*, 367. [CrossRef] [PubMed]
3. Boukraa, R.; Mattana, G.; Battaglini, N.; Piro, B. A Complementary Reduced Graphene Oxide-Based Inverter for Ion Sensing. *Eng. Proc.* **2022**, *16*, 2. [CrossRef]
4. Ramalingam, M.; Jaisankar, A.; Cheng, L.; Krishnan, S.; Lan, L.; Hassan, A.; Sasmazel, H.T.; Kaji, H.; Deigner, H.-P.; Pedraz, J.L.; et al. Impact of nanotechnology on conventional and artificial intelligence-based biosensing strategies for the detection of viruses. *Discov. Nano* **2023**, *18*, 1–28. [CrossRef] [PubMed]
5. Macchia, E.; Torsi, L. Biochemical Sensing, in Introduction to Bioelectronics: Materials, devices, applications. *AIP Publ.* **2022**, 5-1–5-22. [CrossRef]
6. Shaposhnik, P.A.; Poimanova, E.Y.; Abramov, A.A.; Trul, A.A.; Anisimov, D.S.; Kretova, E.A.; Agina, E.V.; Ponomarenko, S.A. Applying of C8-BTBT-Based EGOFETs at Different pH Values of the Electrolyte. *Chemosensors* **2023**, *11*, 74. [CrossRef]
7. Liu, N.; Chen, R.; Wan, Q. Recent Advances in Electric-Double-Layer Transistors for Bio-Chemical Sensing Applications. *Sensors* **2019**, *19*, 3425. [CrossRef]
8. Cramer, T.; Kyndiah, A.; Murgia, M.; Leonardi, F.; Casalini, S.; Biscarini, F. Double layer capacitance measured by organic field effect transistor operated in water. *Appl. Phys. Lett.* **2012**, *100*, 143302. [CrossRef]

9.　Macchia, E.; Torricelli, F.; Bollella, P.; Sarcina, L.; Tricase, A.; Di Franco, C.; Österbacka, R.; Kovács-Vajna, Z.M.; Scamarcio, G.; Torsi, L. Large-Area Interfaces for Single-Molecule Label-free Bioelectronic Detection. *Chem. Rev.* **2022**, *122*, 4636–4699. [CrossRef]

10.　Poimanova, E.Y.; Shaposhnik, P.A.; Anisimov, D.S.; Zavyalova, E.G.; Trul, A.A.; Skorotetcky, M.S.; Borshchev, O.V.; Vinnitskiy, D.Z.; Polinskaya, M.S.; Krylov, V.B.; et al. Biorecognition Layer Based On Biotin-Containing [1]Benzothieno[3,2-b][1]benzothiophene Derivative for Biosensing by Electrolyte-Gated Organic Field-Effect Transistors. *ACS Appl. Mater. Interfaces* **2022**, *14*, 16462–16476. [CrossRef]

11.　Arlett, J.L.; Myers, E.B.; Roukes, M.L. Comparative advantages of mechanical biosensors. *Nat. Nanotechnol.* **2011**, *6*, 203–215. [CrossRef]

12.　Samuel, V.R.; Rao, K.J. A review on label free biosensors. *Biosens. Bioelectron. X* **2022**, *11*, 100216. [CrossRef]

13.　Macchia, E.; Giordano, F.; Magliulo, M.; Palazzo, G.; Torsi, L. An analytical model for bio-electronic organic field-effect transistor sensors. *Appl. Phys. Lett.* **2013**, *103*, 103301. [CrossRef]

14.　Ni, S.; Zhuo, Z.; Pan, Y.; Yu, Y.; Li, F.; Liu, J.; Wang, L.; Wu, X.; Li, D.; Wan, Y.; et al. Recent progress in aptamer discoveries and modifications for therapeutic applications. *ACS Appl. Mater. Interfaces* **2021**, *13*, 9500–9519. [CrossRef] [PubMed]

15.　Shaban, S.M.; Kim, D.-H. Recent advances in aptamer sensors. *Sensors* **2021**, *21*, 979. [CrossRef] [PubMed]

16.　Chakraborty, B.; Das, S.; Gupta, A.; Xiong, Y.T.-V.V.; Kizer, M.E.; Duan, J.; Chandrasekaran, A.R.; Wang, X. Aptamers for Viral Detection and Inhibition. *ACS Infect. Dis.* **2022**, *8*, 667–692. [CrossRef] [PubMed]

17.　Kim, J.; Noh, S.; Park, J.A.; Park, S.-C.; Park, S.J.; Lee, J.-H.; Ahn, J.-H.; Lee, T. Recent Advances in Aptasensor for Cytokine Detection: A Review. *Sensors* **2021**, *21*, 8491. [CrossRef] [PubMed]

18.　Ambartsumyan, O.; Gribanyov, D.; Kukushkin, V.; Kopylov, A.; Zavyalova, E. SERS-based biosensors for virus determination with oligonucleotides as recognition elements. *Int. J. Mol. Sci.* **2020**, *21*, 3373. [CrossRef]

19.　Lou, B.; Liu, Y.; Shi, M.; Chen, J.; Li, K.; Tan, Y.; Chen, L.; Wu, Y.; Wang, T.; Liu, X.; et al. Aptamer-based biosensors for virus protein detection. *Trends Analyt. Chem.* **2022**, *157*, 116738. [CrossRef]

20.　Kukushkin, V.; Kristavchuk, O.; Andreev, E.; Meshcheryakova, N.; Zaborova, O.; Gambaryan, A.; Nechaev, A.; Zavyalova, E. Aptamer-coated track-etched membranes with a nanostructured silver layer for single virus detection in biological fluids. *Front. Bioeng. Biotechnol.* **2023**, *10*, 1076749. [CrossRef]

21.　Yuan, Y.; Giri, G.; Ayzner, A.L.; Zoombelt, A.P.; Mannsfeld, S.C.B.; Chen, J.; Nordlund, D.; Toney, M.F.; Huang, J.; Bao, Z. Ultra-high mobility transparent organic thin film transistors grown by an off-centre spin-coating method. *Nat. Commun.* **2014**, *5*, 3005. [CrossRef]

22.　Zhang, Q.; Leonardi, F.; Casalini, S.; Temiño, I.; Mas-Torrent, M. High performing solution-coated electrolyte-gated organic field-effect transistors for aqueous media operation. *Sci. Rep.* **2016**, *6*, 1–10. [CrossRef]

23.　Shaposhnik, P.A.; Anisimov, D.A.; Trul, A.A.; Agina, E.V.; Ponomarenko, S.A. A Simple Approach to Fabrication of Highly Efficient Electrolyte-Gated Organic Transistors by Phase Microsegregation of 2,7-Dioctyl [1]Benzothieno[3,2-b]Benzothiophene and Polystyrene Mixtures. *Dokl. Phys. Chem.* **2021**, *496*, 20–24. [CrossRef]

24.　Xie, P.; Liu, T.; Sun, J.; Yang, J. Structures, Properties, and Device Applications for [1]Benzothieno[3,2-b]Benzothiophene Derivatives. *Adv. Funct. Mater.* **2022**, *32*, 2200843. [CrossRef]

25.　Anisimov, D.S.; Chekusova, V.P.; Trul, A.A.; Abramov, A.A.; Borshchev, O.V.; Agina, E.V.; Ponomarenko, S.A. Fully Integrated Ultra-Sensitive Electronic Nose Based on Organic Field-Effect Transistors. *Sci. Rep.* **2021**, *11*, 1–12. [CrossRef] [PubMed]

26.　Bayn, A.; Feng, X.; Müllen, K.; Haick, H. Field-efect transistors based on polycyclic aromatic hydrocarbons for the detection and classifcation of volatile organic compounds. *ACS Appl. Mater.* **2013**, *5*, 3431–3440. [CrossRef]

27.　Zhavnerko, G.; Marletta, G. Developing Langmuir–Blodgett strategies towards practical devices. *Mater. Sci. Eng.* **2010**, *169*, 43–48. [CrossRef]

28.　Shiratori, I.; Akitomi, J.; Boltz, D.A.; Horii, K.; Furuichi, M.; Waga, I. Selection of DNA aptamers that bind to influenza A viruses with high affinity and broad subtype specificity. *Biochem. Biophys. Res. Commun.* **2014**, *443*, 37–41. [CrossRef]

29.　Pang, Y.; Rong, Z.; Wang, J.; Xiao, R.; Wang, S. A fluorescent aptasensor for H5N1 influenza virus detection based-on the core-shell nanoparticles metal-enhanced fluorescence (MEF). *Biosens. Bioelectron.* **2015**, *66*, 527–532. [CrossRef]

30.　Zou, X.; Wu, J.; Gu, J.; Shen, L.; Mao, L. Application of Aptamers in Virus Detection and Antiviral Therapy. *Front. Microbiol.* **2019**, *10*, 1–20. [CrossRef]

31.　Chan, K.-H.; To, K.K.W.; Chan, J.F.W.; Li, C.P.Y.; Chen, H.; Yuen, K.-Y. Analytical Sensitivity of Seven Point-of-Care Influenza Virus Detection Tests and Two Molecular Tests for Detection of Avian Origin H7N9 and Swine Origin H3N2 Variant Influenza A Viruses. *J. Clin. Microbiol.* **2013**, *51*, 3160–3161. [CrossRef]

32.　Herrmann, B.; Larsson, C.; Zweygberg, B.W. Simultaneous Detection and Typing of Influenza Viruses A and B by a Nested Reverse Transcription-PCR: Comparison to Virus Isolation and Antigen Detection by Immunofluorescence and Optical Immunoassay (FLU OIA). *J. Clin. Microbiol.* **2001**, *39*, 134–138. [CrossRef] [PubMed]

33.　Chung, H.Y.; Jian, M.J.; Chang, C.K.; Lin, J.C.; Yeh, K.M.; Chen, C.W.; Chiu, S.K.; Wang, Y.H.; Liao, S.J.; Li, S.Y.; et al. Novel dual multiplex real-time RT-PCR assays for the rapid detection of SARS-CoV-2, influenza A/B, and respiratory syncytial virus using the BD MAX open system. *Emerg. Microbes Infect.* **2021**, *10*, 161–166. [CrossRef] [PubMed]

34.　Luo, S.; Xie, Z.; Xie, L.; Liu, J.; Xie, Z.; Deng, X.; Huang, L.; Huang, J.; Zeng, T.; Khan, M.I. Reverse-transcription, loop-mediated isothermal amplification assay for the sensitive and rapid detection of H10 subtype avian influenza viruses. *Virol. J.* **2015**, *12*, 1–7. [CrossRef]

35.   Tsang, T.K.; Cowling, B.J.; Fang, V.J.; Chan, K.H.; Ip, D.K.; Leung, G.M.; Peiris, J.S.; Cauchemez, S. Influenza A Virus Shedding and Infectivity in Households. *J. Infect. Dis.* **2015**, *212*, 1420–1428. [CrossRef] [PubMed]

36.   Doumbia, A.; Webb, M.; Behrendt, M.; Wilson, R.; Turner, M. Robust Microfluidic Integrated Electrolyte-Gated Organic Field-Effect Transistor Sensors for Rapid, In Situ and Label-Free Monitoring of DNA Hybridization. *Adv. Electron. Mater.* **2022**, *8*, 2200142. [CrossRef]

37.   Macchia, E.; Kovács-Vajna, Z.M.; Loconsole, D.; Sarcina, L.; Redolfi, M.; Chironna, M.; Torricelli, F.; Torsi, L. A Handheld Intelligent Single-Molecule Binary Bioelectronic System for Fast and Reliable Immunometric Point-of-Care Testing. *Sci. Adv.* **2022**, *8*, eabo0881. [CrossRef]